



Organic light-emitting transistors with a thin metal layer covering a diffraction grating

Yuki Obama, Yusaku Sakurai, Takenori Kitazawa, Takeshi Yamao & Shu Hotta

To cite this article: Yuki Obama, Yusaku Sakurai, Takenori Kitazawa, Takeshi Yamao & Shu Hotta (2016) Organic light-emitting transistors with a thin metal layer covering a diffraction grating, *Molecular Crystals and Liquid Crystals*, 629:1, 218-223, DOI: 10.1080/15421406.2015.1095833

To link to this article: <http://dx.doi.org/10.1080/15421406.2015.1095833>



Published online: 16 Jun 2016.



Submit your article to this journal [↗](#)



Article views: 34



View related articles [↗](#)



View Crossmark data [↗](#)

Organic light-emitting transistors with a thin metal layer covering a diffraction grating

Yuki Obama, Yusaku Sakurai¹, Takenori Kitazawa, Takeshi Yamao, and Shu Hotta

Department of Macromolecular Science and Engineering, Kyoto Institute of Technology, Matsugasaki, Sakyo-ku, Kyoto, Japan

ABSTRACT

We fabricated organic light-emitting transistors (OLETs) characterized by an Ag layer deposited on a one-dimensional (1D) or two-dimensional (2D) diffraction grating that acts as a combined gate insulator with SiO₂. The Ag layer was entirely covered with an organic crystal. Upon photoexcitation that crystal showed narrow linewidth emissions (NLEs) parallel to the substrate plane. The narrowed lines were either redshifted or blueshifted with rotation of the crystal around a normal to its surface with respect to the grating wave vector. Strong emissions ($\sim 10^4$ – 10^6 cd m⁻²) accompanied by current-injected NLEs were observed from the 1D and 2D grating OLETs.

KEYWORDS



Organic light-emitting transistors; thiophene/phenylene co-oligomer; diffraction gratings; organic crystals

Introduction

Since Hepp et al. presented organic light-emitting transistors (OLETs) [1], many researches have been carried out to achieve bright emission and high efficiency on the OLETs. To promote simultaneous injections of both electrons and holes into an organic layer, multilayers composed of e.g. p- and n-type organic semiconductors can be employed as emission layers [2,3]. Recently, we developed novel OLETs characterized by a metal oxide semiconductor layer inserted between an organic thin film and a gate insulator layer [4,5]. Using these devices we succeeded in obtaining bright light emission at relatively low voltages ($\sim \pm 20$ V).

Meanwhile, narrow linewidth emissions (NLEs) have been pursued in the organic devices for the purpose of current-injected laser oscillations [6]. In this context, we formed one-dimensional (1D) and two-dimensional (2D) diffraction gratings on the surface of gate insulator layers of OLETs made of organic crystals [7–9]. In fact these devices showed current-injected NLEs with their full-widths at half maximum (FWHMs) down to 2.1 nm.

In the present studies, we combined a 1D or 2D diffraction grating with a thin Ag layer deposited on it. As an organic material, we chose a crystal of 1,4-bis{5-[4-(2'-thienyl)phenyl]thiophen-2-yl}benzene [abbreviated as AC7, see Fig. 1(a)], one of thiophene/phenylene co-oligomers [10]. We observed intense emissions with the maximum

CONTACT Takeshi Yamao  yamao@kit.ac.jp  Department of Macromolecular Science and Engineering, Kyoto Institute of Technology, Matsugasaki, Sakyo-ku, Kyoto 606-8585, Japan.

¹Present address: Harima Chemicals, Inc., Noguchi-cho, Kakogawa, Hyogo 675-0019, Japan

Color versions of one or more of the figures in the article can be found online at www.tandfonline.com/gmcl.

This paper was originally submitted to *Molecular Crystals and Liquid Crystals*, Volumes 620–622, Proceedings of the KJF International Conference on Organic Materials for Electronics and Photonics 2014.

© 2016 Taylor & Francis Group, LLC

luminance of $\sim 10^6$ cd m $^{-2}$ from these OLETs. Of these, the OLET having the 2D diffraction grating produced current-injected NLEs.

Experiments

We used an Si wafer covered with a 300-nm-thick SiO $_2$ layer for a substrate. We fabricated the 1D diffraction grating on the surface of a MicroChem SU-8 2000.5 photoresist film spin-coated on the substrate (3000 rpm, 30 s). We first baked the film at 65 and 95°C for 10–15 min each, and formed the diffraction grating by interference exposure with the Lloyd mirror setup [7,11]. An exposure source was the third harmonic generation of an Nd:YAG laser (wavelength: 355 nm, pulse duration: 18 ns, repetition rate: 10 Hz, beam diameter: 4 mm, pulse energy: 30–40 μ J). The incidence angle of the Lloyd mirror was set to 20.7–20.9° from the direction normal to the film surface. After exposure for 16–30 s, we baked it again at 65 and 95°C for 10 min each. The film was then developed, rinsed with 2-propanol and dried. We further baked the film at 175°C for 25 min. The period and depth of the grooves were 483–530 nm and 62–113 nm, respectively.

The 2D diffraction grating (SCIVAX Corporation, RSLH230/200–4) was fabricated using the nanoimprint lithography. Circular air holes formed a triangular lattice on a cyclic polyolefin resist layer that covered the substrate. The pitch, diameter, and depth of holes were 480, 238, and 225 nm, respectively.

We deposited a 50-nm-thick Ag layer in vacuum through a mask on the gratings. Figures 1(b) and (c) show atomic force microscope (AFM) images of the 1D and 2D grating surfaces after Ag deposition along with a grating wave vector and the Brillouin zone with high-symmetry points (Γ , M, K), respectively.

AC7 crystals were grown by the vapor phase method using a sublimation recrystallization apparatus made of two heaters (source and growth heaters) and a glass test tube including glass cylinders that fit inside the test tube [12,13]. We set the source and growth heater temperatures at 360 and 320°C, respectively, and maintained them for 20 h. We choked the outlet side of the test tube with silica wool [13]. We picked up the grown crystals that stood on the inside wall of the glass cylinders with a hair of a brush. We laminated them on the gratings to completely cover the Ag layer and the crystals were electrostatically adsorbed on the surface of the gratings.

Figure 1(d) shows a schematic cross-section of the OLET. We fabricated an alloy layer (15 nm) of Mg and Ag, Ag (50 nm) and Au (100 nm) layers on the crystal using the same setup as before [14]. We term the left-hand (right-hand) electrode an Au (MgAg) electrode. The channel length and width were 14–15 μ m and 700–780 μ m, respectively. The angle between the direction along the channel width and the grating wave vector (Γ –M direction) was -5.4°

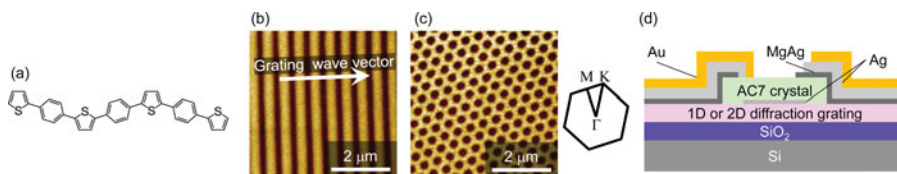


Figure 1. (a) Structural formula of AC7. AFM images of the (b) 1D and (c) 2D grating surfaces on which Ag was deposited. Diagrams (b) and (c) include a grating wave vector and the Brillouin zone with high-symmetry points (Γ , M, K) in the reciprocal lattice, respectively. (d) Schematic cross-section of the OLET with the grating.

(-5.9°) in the 1D (2D) grating device [see Figs. 1(b) and (c)]. The grating formed a gate insulator together with the SiO_2 layer. The Si was used as the gate contact.

We measured the photoexcited emission spectra of an AC7 crystal on the 1D grating before electrode fabrication with the same setup as before [15]. We excited two parts on the crystal with and without the Ag layer on the grating through an objective lens ($\times 100$) with unpolarized violet light (380–420 nm). We measured the spectra parallel to the crystal plane as functions of the rotation angle with respect to the direction of the grating wave vector around the direction normal to the crystal plane [15]. In this geometry, the emission spectra were measured from -90 to $+90^\circ$ by 10° steps. The positive angle means the rotation of the sample in a counterclockwise direction.

We measured current-voltage characteristics under vacuum ($\sim 10^{-3}$ Pa) in the dark. We grounded the Au electrode as the source contact [16]. We measured drain currents of the 1D (2D) grating device under application of direct current (DC) voltages ranging from 5 to -5 V (0 to -100 V) to the drain contact with various DC gate voltages from 60 to -10 V (0 to -100 V).

We observed the current-injected emissions in vacuum ($\sim 10^{-3}$ Pa) by applying positive and negative DC voltages having the same absolute value of 10–190 V to the Au and MgAg electrodes, respectively: The gate contact was grounded [4,5]. We recorded light emissions parallel to the direction along the channel width. We accumulated the emissions for 5 s.

Results and discussion

Figure 2(a) shows the rotation angle dependence of the emission spectra of the AC7 crystal on the 1D grating. For this, we excited the part without the Ag layer. Two narrow emission lines were redshifted with increased absolute values of the rotation angle. The lines were intense at ~ 530 – 570 nm and ~ 640 – 660 nm. Figure 2(b) depicts emission spectra of the AC7 crystal excited on the 1D grating covered with Ag. Weak blueshifted peaks were observed around

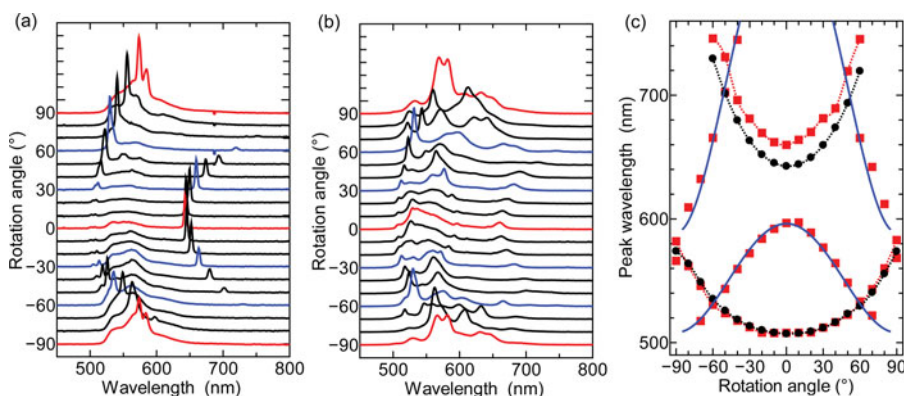


Figure 2. Rotation angle dependence of emission spectra of the AC7 crystal on the 1D grating. We excited the parts of the crystal (a) without and (b) with the Ag layer on the 1D grating. The rotation angles were changed around the direction normal to the crystal plane with respect to the direction of the grating wave vector. To distinguish the spectra, those measured at 0° and $\pm 90^\circ$ ($\pm 30^\circ$ and $\pm 60^\circ$) are plotted as red (blue) curves. (c) Rotation angle dependence of the emission peak wavelengths of the AC7 crystal on the 1D grating. The parts of the crystal without (black circles) and with (red squares) the Ag layer on the grating were excited. Blue solid curves are fitting ones into the simple Bragg–Snell formula for the peak positions blueshifted with the increased absolute value of the rotation angle. Red and black dotted curves are drawn as a guide connecting peak positions that were redshifted with the rotation angle.

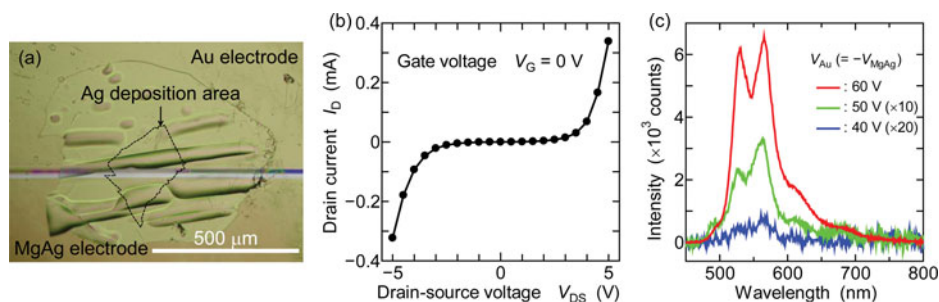


Figure 3. (a) Top-view micrograph of the device made of the AC7 crystal on the Ag-covered 1D grating. The deposition area of Ag is surrounded by the black dotted line. (b) Current-voltage characteristics measured at the gate voltage of 0 V. (c) Current-injected emission spectra measured at applied voltages (V_{Au} and V_{MgAg}) of ± 40 , ± 50 , and ± 60 V to the Au and MgAg electrodes. The spectra measured at ± 40 and ± 50 V were longitudinally magnified by factors of 20 and 10, respectively.

550–600 nm and 560–700 nm along with two redshifted peaks similar to those in Fig. 2(a). The peaks were intense at ~ 530 and ~ 560 nm. The intense peak locations in Figs. 2(a) and (b) are in agreement with emission maxima (around 540, 560, and 610 nm) and a shoulder (around 650 nm) measured along the crystal plane of an unprocessed AC7 crystal.

We resolved the spectra of the AC7 crystal on the 1D grating with and without the Ag layer [see Figs. 2(a) and (b)] into distinct peaks by using pseudo-Voigt functions [17]. We plotted the peak wavelengths as a function of the rotation angle in Fig. 2 (c). The redshifted peaks of the crystal with and without Ag were well accorded with each other within ~ 20 nm. We fitted the blueshifted peaks λ_p into the simple Bragg–Snell formula [18]:

$$m\lambda_p = 2\Lambda\sqrt{n_{\text{eff}}^2 - \sin^2\theta} \quad (1)$$

where m is the diffraction order, Λ is the grating period (515 nm), θ is the angle from the grating wave vector, and n_{eff} is the effective refractive index (assumed to be a constant). The results are blue solid curves in Fig. 2(c). This indicates that the Ag layer increased reflection of light traveling in the crystal.

Figures 3(a) and (b) show a top-view micrograph of the 1D device and its current-voltage characteristics measured at the gate voltage of 0 V, respectively. The drain current flowed at both positive and negative drain-source voltages. At +5 and -5 V those currents were 0.34 and -0.32 mA, respectively. These currents varied within at most $30 \mu\text{A}$ with the gate voltage change from -10 to 60 V. The results resembled those observed in the devices where aluminum-doped zinc oxide layer was inserted between the organic semiconductor and gate insulator layers [4,5].

Figure 3(c) shows current-injected emission spectra. The device started to emit the light at applied voltages of ± 40 V: The average emission intensity from 560 to 570 nm was 36 counts. With increase in voltage, the emission intensity rapidly increased and reached up to 6571 counts at 562.2 nm at applied voltage of ± 60 V. Two major peaks located around 530 and 565 nm were sharper at ± 60 V than at ± 40 and ± 50 V. The former peak seemed to preferentially increase with the applied voltages.

From the spectra in Fig. 3(c), we estimated luminance. For this we used a light emission area ($\sim 1.1 \times 10^{-11} \text{ m}^2$), a distance between the device and a detector (115.5 mm), and a light receiving area of the detector ($\sim 7.9 \times 10^{-7} \text{ m}^2$). We assumed that light emission occurred only at the crystal edge. The luminances were $2.1 \times 10^6 \text{ cd m}^{-2}$ at ± 60 V, $9.6 \times 10^4 \text{ cd m}^{-2}$ at ± 50 V, and $9.7 \times 10^3 \text{ cd m}^{-2}$ at ± 40 V. These values were higher than those of other typical

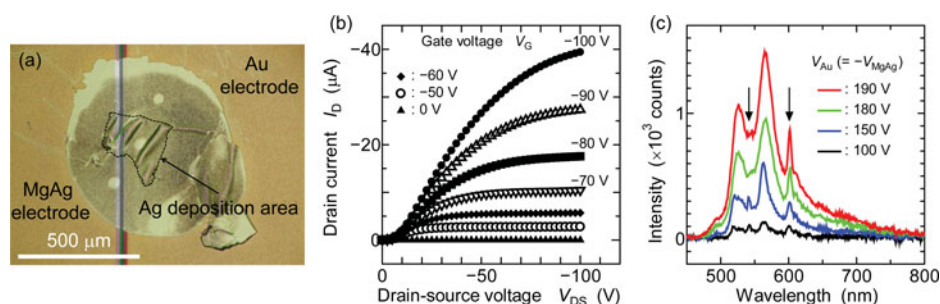


Figure 4. (a) Top-view micrograph of the device made of the AC7 crystal on the Ag-covered 2D grating. The deposition area of Ag is surrounded by the black dotted line. (b) Output characteristics of the device. (c) Current-injected emission spectra measured at applied voltages (V_{Au} and V_{MgAg}) from ± 100 to ± 190 V to the Au and MgAg electrodes. The two arrows indicate the NLE positions.

Table 1. Fitted peak positions and their full-widths at half maxima (FWHMs) of the current-injected emissions from the OLET of the AC7 crystal on the Ag-covered 2D grating. V_{Au} indicates the applied voltage to the Au electrode.

V_{Au} (V)	Peak position (FWHM) (nm)				
100	522.9 (18.3)	542.1 (5.7)	564.1 (18.6)	601.6 (12.4)	
150	523.9 (19.3)	541.7 (7.0)	563.1 (13.9)	602.0 (6.8)	
180	525.8 (21.4)	544.0 (12.8)	565.9 (28.1)	601.8 (4.9)	
190	525.2 (18.0)	— ^a	566.7 (26.5)	601.6 (4.8)	

^a Fitted data are not shown due to low reliability.

OLETs without the grating or an inorganic interlayer between the organic emission layer and the insulator layer ($\sim 10^2$ – 10^3 cd m⁻²) [19,20].

Figures 4(a) and (b) show a top-view micrograph of the 2D grating device and its output characteristics, respectively. In contrast to the 1D grating device, this device indicated normal characteristics of a p-type organic field-effect transistor. The drain currents were saturated at larger absolute values of drain-source voltages than those of gate voltages, even though these increased nonlinearly from the origin [21]. We estimated the hole mobilities at 9.32×10^{-2} and 2.38×10^{-2} cm² V⁻¹ s⁻¹ in the saturation and linear regions, respectively.

Figure 4(c) shows current-injected emission spectra. Two sharp peaks were observed around 540 and 600 nm [indicated by the arrows in Fig. 4(c)]. We resolved the spectra into peaks and summarize them in Table 1. The 540-nm line (located at 541.7–544.0 nm) was pronounced and sharp at lower voltage magnitudes (100 and 150 V) and became unnoticeable at larger magnitudes (190 V). The 600-nm line (601.6–602.0 nm) increased and became sharp with the voltage magnitudes. The 600-nm line as well as the 540-nm line was NLE under current-injection.

Conclusions

We have fabricated OLETs made of an organic oligomer AC7 crystal combined with an Ag layer deposited on a 1D or 2D diffraction grating. The crystal was laminated on the grating to thoroughly cover the Ag layer. Upon photoexcitation, NLEs were observed from the crystal on the Ag-covered 1D grating. These lines were redshifted or blueshifted with rotation of the crystal around a normal to its surface with respect to the grating wave vector. Only redshifted lines were observed when we optically excited a part of the crystal without Ag on the grating. The Ag layer seemed effective in the reflection of the light traveling in the crystal.

The 1D grating OLET showed the current-voltage characteristics similar to those observed in the OLETs with an intervening metal oxide semiconductor layer between the organic and gate insulator layers [4,5]. The 1D grating device showed strong emissions with the maximum luminance of $\sim 10^6$ cd m $^{-2}$ under current injection. The 2D grating OLET depicted normal p-type transistor characteristics with a hole mobility of $\sim 10^{-1}$ – 10^{-2} cm 2 V $^{-1}$ s $^{-1}$ and produced current-injected NLEs. The present results indicate the potential for the bright NLEs under current injection by using the combination of the diffraction grating and the metal layer.

Acknowledgments

This work was supported by Grants-in-Aid for Scientific Research A (Grant No. 25248045) and C (Grant No. 23550208) and Challenging Exploratory Research (Grant No. 24655173) from Japan Society for the Promotion of Science (JSPS). The authors thank SCIVAX Corporation for preparing the 2D gratings on the substrate.

References

- [1] Hepp, A., Heil, H., Weise, W., Ahles, M., Schmechel, R., & von Seggern, H. (2003). *Phys. Rev. Lett.*, **91**, 157406.
- [2] Capelli, R., Toffanin, S., Generali, G., Usta, H., Facchetti, A., & Muccini, M. (2010). *Nat. Mater.*, **9**, 496.
- [3] Dinelli, F., Capelli, R., Loi, M. A., Murgia, M., Muccini, M., Facchetti, A., & Marks, T. J. (2006). *Adv. Mater.*, **18**, 1416.
- [4] Yamada, K., Yamao, T., & Hotta, S. (2013). *Adv. Mater.*, **25**, 2860.
- [5] Higashihara, S., Yamada, K., Yamao, T., & Hotta, S. (2014). *Jpn. J. Appl. Phys.*, **53**, 05FT01.
- [6] Samuel, I. D. W., Namas, E. B., & Turnbull, G. A. (2009). *Nat. Photonics*, **3**, 546.
- [7] Makino, Y., Hinode, T., Okada, A., Yamao, T., Tsutsumi, N., & Hotta, S. (2011). *Phys. Procedia*, **14**, 177.
- [8] Makino, Y., Okada, A., Hotta, S., & Yamao, T. (2012). *Mol. Cryst. Liq. Cryst.*, **566**, 8.
- [9] Okada, A., Makino, Y., Hotta, S., & Yamao, T. (2012). *Phys. Status Solidi C*, **9**, 2545.
- [10] Hotta, S., & Katagiri, T. (2003). *J. Heterocycl. Chem.*, **40**, 845.
- [11] Yamao, T., Inoue, T., Okuda, Y., Ishibashi, T., Hotta, S., & Tsutsumi, N. (2009). *Synth. Met.*, **159**, 889.
- [12] Yamao, T., Ota, S., Miki, T., Hotta, S., & Azumi, R. (2008). *Thin Solid Films*, **516**, 2527.
- [13] Fukaya, Y., Inoue, A., Fukunishi, Y., Hotta, S., & Yamao, T. (2013). *Jpn. J. Appl. Phys.*, **52**, 05DC09.
- [14] Yamao, T., Terasaki, K., Shimizu, Y., & Hotta, S. (2010). *J. Nanosci. Nanotechnol.*, **10**, 1017.
- [15] Fukaya, Y., Obama, Y., Hotta, S., & Yamao, T. (2014). *Jpn. J. Appl. Phys.*, **53**, 01AD08.
- [16] Sze, S. M. (1981). *Physics of Semiconductor Devices*, John Wiley & Sons, Inc., New York, U. S. A.
- [17] Heinze, K., Hempel, K., & Beckmann, M. (2006). *Eur. J. Inorg. Chem.*, **2006**, 2040.
- [18] Morandi, V., Marabelli, F., Amendola, V., Meneghetti, M., & Comoretto, D. (2007). *Adv. Funct. Mater.*, **17**, 2779.
- [19] Oyamada, T., Uchiuzou, H., Akiyama, S., Oku, Y., Shimoji, N., Matsushige, K., Sasabe, H., & Adachi, C. (2005). *J. Appl. Phys.*, **98**, 074506.
- [20] Suganuma, N., Shimoji, N., Oku, Y., Okuyama, S., & Matsushige, K. (2008). *Org. Electron.*, **9**, 834.
- [21] Hotta, S., & Yamao, T. (2011). *J. Mater. Chem.*, **21**, 1295.